Dynamic aberrances of substantia nigra-relevant coactivation patterns in first-episode treatment-naïve patients with schizophrenia

Corresponding author:
Tao Li;
Email: litaozjusc@zju.edu.cn

Lihong Deng[1,2,3,4,5,*] ![ORCID], Wei Wei[1,2,3,4,*], Chunxia Qiao[5], Yubing Yin[5], Xiaojing Li[1,2,3,4], Hua Yu[1,2,3,4], Lingqi Jian[5], Xiaohong Ma[5], Liansheng Zhao[5], Qiang Wang[5], Wei Deng[1,2,3,4], Wanjun Guo[1,2,3,4] and Tao Li[1,2,3,4] ![ORCID]

[1]Department of Neurobiology, Affiliated Mental Health Center & Hangzhou Seventh People's Hospital, Zhejiang University School of Medicine, Hangzhou, Zhejiang, China; [2]Nanhu Brain-computer Interface Institute, Hangzhou, Zhejiang, China; [3]Liangzhu Laboratory, MOE Frontier Science Center for Brain Science and Brain-machine Integration, State Key Laboratory of Brain-machine Intelligence, Zhejiang University, Hangzhou, Zhejiang, China; [4]NHC and CAMS Key Laboratory of Medical Neurobiology, Zhejiang University, Hangzhou, Zhejiang, China and [5]Mental Health Center and Psychiatric Laboratory, State Key Laboratory of Biotherapy, West China Hospital of Sichuan University, Chengdu, Sichuan, China

Abstract

Background. Although dopaminergic disturbances are well-known in schizophrenia, the understanding of dopamine-related brain dynamics remains limited. This study investigates the dynamic coactivation patterns (CAPs) associated with the substantia nigra (SN), a key dopaminergic nucleus, in first-episode treatment-naïve patients with schizophrenia (FES).

Methods. Resting-state fMRI data were collected from 84 FES and 94 healthy controls (HCs). Frame-wise clustering was implemented to generate CAPs related to SN activation or deactivation. Connectome features of each CAP were derived using an edge-centric method. The occurrence for each CAP and the balance ratio for antagonistic CAPs were calculated and compared between two groups, and correlations between temporal dynamic metrics and symptom burdens were explored.

Results. Functional reconfigurations in CAPs exhibited significant differences between the activation and deactivation states of SN. During SN activation, FES more frequently recruited a CAP characterized by activated default network, language network, control network, and the caudate, compared to HCs ($F = 8.54$, FDR-$p = 0.030$). Moreover, FES displayed a tilted balance towards a CAP featuring SN-coactivation with the control network, caudate, and thalamus, as opposed to its antagonistic CAP ($F = 7.48$, FDR-$p = 0.030$). During SN deactivation, FES exhibited increased recruitment of a CAP with activated visual and dorsal attention networks but decreased recruitment of its opposing CAP ($F = 6.58$, FDR-$p = 0.034$).

Conclusion. Our results suggest that neuroregulatory dysfunction in dopaminergic pathways involving SN potentially mediates aberrant time-varying functional reorganizations in schizophrenia. This finding enriches the dopamine hypothesis of schizophrenia from the perspective of brain dynamics.

Introduction

Schizophrenia is a severe and often chronic mental disorder characterized by positive symptoms, negative symptoms, and cognitive deficits, affecting approximately 1% of the global population and resulting in substantial economic burden (Charlson et al., 2018; Cloutier et al., 2016; Marder, Ropper, & Cannon, 2019). The dopamine hypothesis has been a primary concern in the pathophysiology of schizophrenia (Howes & Kapur, 2009; McKenna, 1987), suggesting that the neuromodulatory dysfunction in dopaminergic pathways leads to widespread brain dysconnection in schizophrenia (Friston, Brown, Siemerkus, & Stephan, 2016) and contributes to the genesis of psychotic symptoms (Howes, McCutcheon, Owen, & Murray, 2017; Owen, Sawa, & Mortensen, 2016). Substantia nigra (SN), a key dopaminergic nucleus, is structurally and functionally connected with other subcortical structures and extensive cortical areas (Bär et al., 2016; Chinta & Andersen, 2005; Conio et al., 2020). Previous studies have shown elevated dopamine synthesis capacity of SN in schizophrenia and its link to clinical symptoms (Howes et al., 2013). Recent *in vivo* imaging advances demonstrated that dopaminergic dysfunction in schizophrenia is most significant in the nigrostriatal rather than the mesolimbic pathway (McCutcheon, Abi-Dargham, & Howes, 2019; McCutcheon, Beck, Jauhar, & Howes, 2018). This suggests nigral dysfunction may underlie the neuropathological mechanism of schizophrenia.

To date, only a limited number of resting-state functional magnetic resonance imaging (rs-fMRI) studies have investigated the influence of SN on the functional organization of the brain in schizophrenia. Conio et al., suggested that the hyperactive dopamine signaling in SN may lead to overactivity in sensorimotor network (SMN) and salience network (SAN), along with concurrent underactivity in the default mode network (DMN) (Conio et al., 2020). This imbalance in network activity may contribute to the development of psychotic symptoms (Conio et al., 2020). Recent functional connectivity (FC) research on schizophrenia has identified aberrations in striato-thalamo-cortical FC related to SN (Martino et al., 2018). However, partly due to a significant shortage of dynamic information on generated connectivity patterns, the mechanistic interpretation of 'static' rs-fMRI research remains limited (Sporns, Tononi, & Kötter, 2005).

The human brain is a highly dynamic system, operating on multiple spatial and temporal scales even when no specific task is being performed (Chang & Glover, 2010; Hutchison et al., 2013). The coactivation pattern (CAP) method is a framewise dynamic approach specifically designed for analyzing rs-MRI data, allowing for the capture of transient brain organizations (Liu & Duyn, 2013; Liu, Zhang, Chang, & Duyn, 2018). CAPs can be generated through temporal clustering of rs-fMRI frames (i.e. time points or volumes), representing recurrent activity patterns observed during scanning. These CAPs enable us to conduct spatial and temporal dynamic analyses, potentially uncovering evidence for etiopathological mechanisms of schizophrenia that go beyond the scope of stationary FC characterizations (Chen, Chang, Greicius, & Glover, 2015; Christoff, Irving, Fox, Spreng, & Andrews-Hanna, 2016; Liu & Duyn, 2013). Individuals with subthreshold psychotic experiences displayed reduced recruitment of a CAP encompassing SAN and visual network (VIS) compared to healthy controls (HCs) (Wang et al., 2021). This reduction was negatively correlated with the severity of psychotic experiences (Wang et al., 2021). In chronic schizophrenia, temporal dynamic abnormalities extended to more CAPs, including a lower occurrence in a CAP featuring frontoparietal network and SMN and higher occurrence in a CAP involving DMN and SAN (Wang et al., 2021; Yang et al., 2021). A recent CAP study found coactivation between the SAN and basal ganglia networks in prepsychosis, which may suggest the involvement of the dopaminergic pathway (Bolton et al., 2020c). However, the exploratory, whole-brain approach adopted by most CAP studies limited the in-depth investigation of dopaminergic neuromodulation in brain dynamics. Additionally, most CAP studies have been conducted in either schizophrenic patients with lengthy disease courses or individuals at clinical high risks for schizophrenia, which may be affected by medication effects and disease progressions (Vita, De Peri, Deste, & Sacchetti, 2012; Vita, De Peri, Deste, Barlati, & Sacchetti, 2015; Zhang et al., 2018). As a result, there is a need for directly investigating SN-relevant CAPs in the early stage of unmedicated schizophrenia.

The primary objective of this study is to explore the dopamine hypothesis of schizophrenia from a dynamic perspective. We have focused on the dopaminergic SN as a seed region to reveal temporal dynamic features of SN-relevant brain CAPs in first-episode treatment-naïve patients with schizophrenia (FES) and HCs. These features are characterized by the occurrence of each CAP and the balance between antagonistic CAPs. Additionally, to illustrate the spatial features of each CAP, we have described their activity characteristics and derived their connectome profiles using a novel edge-centric method (Sporns, Faskowitz, Teixeira,

Cutts, & Betzel, 2021). Moreover, we investigated the correlations between aberrant dynamics and symptom burden in FES. In light of the dopamine hypothesis and supporting evidence, we propose that there will be observable temporal and spatial dynamic aberrances in CAPs, coupled with either the activation or deactivation of the SN, particularly in the early stage of schizophrenia.

Methods

Participants

A total of 86 FES and 97 age- and gender-matched HCs were recruited from the Mental Health Center of West China Hospital, Sichuan University, from October 2014 to June 2018 in this study. Details are provided in the online Supplement. The severity of symptoms was rated by the Positive and Negative Syndrome Scale (PANSS) (Kay, Fiszbein, & Opler, 1987). A consensus five-factor model of the PANSS was adopted, including Positive, Negative, Disorganized/Concrete, Excited, and Depressed factors (Wallwork, Fortgang, Hashimoto, Weinberger, & Dickinson, 2012). The short version of the Wechsler Adult Intelligence Scale-Revised in China (WAIS-RC) was used to evaluate intelligence quotient (IQ) (Gong & Dai, 1984; Schopp, Callahan, Johnstone, & Schwake, 1998). Written informed consent was obtained from all participants or their legal guardians after explaining the research. This study was approved by the Institutional Review Board of West China Hospital of Sichuan University and in accordance with the Helsinki Declaration.

MRI data acquisition

All scanning was performed on a Philips 3.0 T MR scanner (Achieva, TX, best, Amsterdam, the Netherlands) with an eight-channel phased-array head coil. The rs-fMRI images were collected by using a gradient-echo echo-planar imaging sequence with the following parameters: repetition time 2000 ms, echo time 30 ms, flip angle = 90°, slice thickness 4.0 mm with no slice gap, matrix size 64×64, field of view 240×240 mm^2, reconstructed voxel size $3.75 \times 3.75 \times 4$ mm^3, and 38 slices. Each functional run contained 240 volumes and lasted for 8 min and 6 s. See the scanning details in the Supplement.

Imaging preprocessing

Data preprocessing was performed using the Data Processing Assistant for Resting-State fMRI (DPARSF) software suite (http://rfmri.org/DPARSF) (Yan & Zang, 2010). Standard preprocessing was performed, including the following steps: removing the first 10 time points, slice timing correction, realignment, co-registration, T1 segmentation, normalization, nuisance regression (including head motion, mean white matter, mean cerebrospinal fluid signal, and mean global signal), detrending, bandpass filtering (0.01–0.1 Hz), and spatial smoothing using a 6 mm FWHM Gaussian kernel. Details of preprocessing are provided in the Supplement.

To reduce the impact of head motion, we scrubbed the frames with >0.5 mm framewise displacement (FD) (Power, Barnes, Snyder, Schlaggar, & Petersen, 2012). Subjects with a mean FD exceeding 0.5 mm or with more than 30 scrubbed frames were excluded. After quality control, 84 FES and 94 HCs remained. We followed the codes from the TbCAPs toolbox (Bolton et al., 2020b) for this step.

Next, to reduce the dimensionality of the original voxel-wise rs-fMRI data, we extracted the mean blood oxygen level-dependent (BOLD) time series for each cortical region using the Schaefer2018 atlas with 400 cortical parcellations, which are matched to the Kong2022 17 network order (Kong et al., 2021), and that of the subcortex with the Harvard-Oxford subcortical structural atlas with 16 parcels (Desikan et al., 2006). See details of the two atlases in the Supplement. This step was executed in DPARSF.

To determine the relative level of spontaneous neural activity, we standardized the time series of the 416 regions of interest (ROIs) into Z scores. This standardization was essential for our subsequent CAP analyses (Liu et al., 2018). Normalization was carried out using the codes of TbCAPs (Bolton et al., 2020b).

CAP analysis

To investigate the SN-coupled CAPs, the SN was chosen as a seed region for a seed-based CAP approach. For extracting the mean BOLD signal of the SN, we utilized a bilateral 7 T MRI SN mask from the ATAG-Atlas (https://www.nitrc.org/projects/atag), which allowed us to accurately capture the SN's activity (Keuken et al., 2014).

Prior to clustering analysis, time points with SN activity intensity among the top 20% (approximately 46 time points) and the bottom 20% were extracted separately. The intensity threshold (20%) was chosen to ensure that we could capture the dynamic variability of the brain (Chen et al., 2015; Liu & Duyn, 2013). A resampling-based consensus clustering method (Monti, Tamayo, Mesirov, & Golub, 2003), which is regarded as particularly effective in the condition of dimensionally large datasets, was implemented to classify the extracted time points at the population level. Clustering was performed for the time points coupled with SN activation and deactivation, respectively, using the spherical k-means clustering algorithm with the R package 'cola' (Gu, Schlesner, & Hübschmann, 2021). The consensus of optimal cluster number was voted according to the silhouette score (Rousseeuw, 1987) and the proportion of ambiguously clustered pairs (Şenbabaoğlu, Michailidis, & Li, 2014) of 50 times repeated clustering results. In this study, to balance the clustering validity and stability, the solution of six clusters was exploited for both sets of time points (see details of clustering analyses in the Supplement and cluster validation in online Supplementary Fig. S1). Each cluster referred to a transient brain activity state that recurred during SN activation or SN deactivation. Finally, time points in the same cluster were averaged and then spatially Z-scored to generate the activity maps (i.e. CAPs) at the whole population level.

Edge-centric analysis

In our edge-centric approach to depict the connectome profiles of SN-related CAPs, we computed the strength of edges between ROI pairs using the elementwise product for each SN-related frame (Faskowitz, Esfahlani, Jo, Sporns, & Betzel, 2020). Given that the average of edge magnitudes over time equates to the Pearson's correlation coefficient (Faskowitz et al., 2020), we constructed connectome maps for each CAP by averaging the edge profiles from each SN-related frame.

Analysis of spatial features

To test the spatial similarities among all SN-relevant CAPs and their connectome maps, we employed Spearman's correlation tests. This approach allowed us to quantitatively evaluate the degree of similarity in the spatial organization of these CAPs.

To examine group differences in spatial features, we generated CAPs and corresponding connectome maps for each group and also created individual-level CAPs. Initially, we evaluated the spatial similarities between group-level CAPs and connectome maps of the two groups using Spearman's correlations. Subsequently, we conducted two-sample t tests comparing individual-level CAPs between the groups. We applied false discovery rate (FDR) correction to the p values, considering FDR-corrected $p < 0.05$ as statistically significant.

Calculation of temporal dynamic metrics

To illustrate the temporal features of CAPs, we calculated the occurrence of each CAP and the balance ratio of antagonistic CAPs for each participant. The occurrence was defined by the times a given CAP emerged, which describes how frequently the CAP recurred during the whole scan. Previous CAP research has discovered that some CAPs displayed opposing spatial patterns, and these CAPs may exhibit competing dynamics (Bolton et al., 2020c; Yang et al., 2021). To assess a potential competing relationship among CAPs, we computed a balance ratio for all pairs of CAPs with opposing activation patterns that we previously identified in spatial similarity tests. The balance ratio was calculated as (CAP_1 occurrences – CAP_2 occurrences) / (CAP_1 occurrences + CAP_2 occurrences). This will yield values between −1 and 1, with a higher absolute value indicating the predominance of CAP_1 (positive values) or CAP_2 (negative values), and a zero-value reflecting the balance between two CAPs.

The dynamic analyses in this study were performed using customized scripts in MATLAB 2017a (MathWorks), except that the clustering analyses were conducted in R 4.0.5. The schematic pipeline of the study design is shown in Fig. 1.

Statistical analysis

Statistical analyses were carried out in SPSS 25.0 (IBM SPSS Statistics). Chi-square tests or two-sample t tests were used to examine the group differences in sex, age, and years of education. One-way analyses of covariance (ANCOVAs) were conducted to test the intergroup difference in temporal features of CAPs and IQ, adjusting for age, gender, and years of education. Then partial correlation tests adjusting for age, sex, and years of education were used to assess the relationship between altered temporal metrics and symptom severity (PANSS total and factor scores). We used Spearman's correlation to evaluate the relationship between temporal dynamics and the duration of untreated psychosis (DUP) after regressing out age, sex, and years of education, as DUP showed a skewed distribution. The FDR corrections were applied to correct multiple comparisons. Statistical significance was set at FDR-corrected $p < 0.05$.

In our statistical analysis, we examined the potential influence of IQ on our findings by including it as an additional confounding factor in the between-group comparisons of temporal features and correlation tests.

Results

Demographic, clinical, and neurocognitive data

The demographic, clinical, and neurocognitive information of all subjects is presented in Table 1. Age and sex did not differ
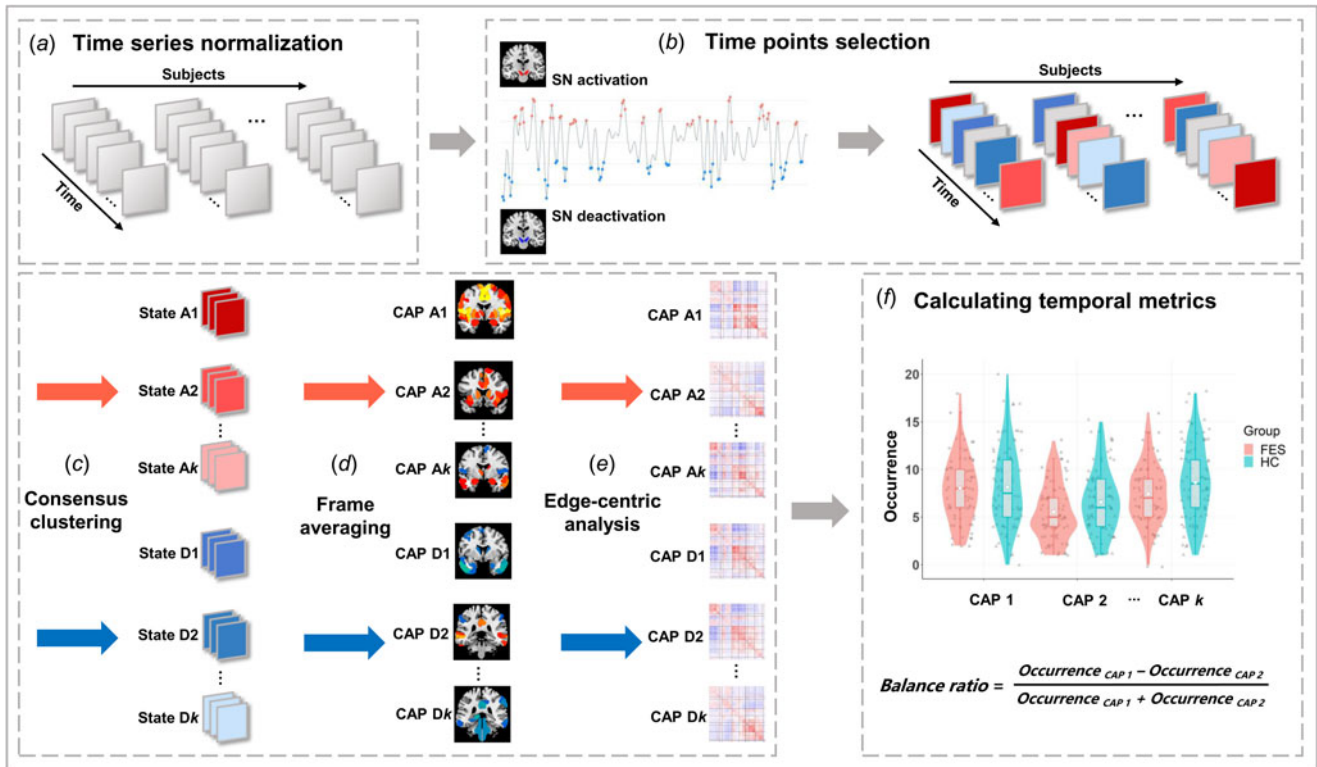
Figure 1. Overall analysis pipeline for this SN-relevant CAP study. We included six main steps: (a) the time series of 416 ROIs and the seed (bilateral SN) were normalized for each participant; (b) time points with SN activity intensity among the top 20% and the bottom 20% were labeled and later extracted separately; (c) consensus clustering was performed to classify activated and deactivated SN coupled time points into k clusters respectively; (d) CAP maps for each state were generated by averaging and spatially Z-scoring the frames within the same cluster; (e) edge-centric analyses were applied to generate the connectome patterns for each CAP; and (f) temporal metrics, the occurrence of each CAP and balance ratio for opposing CAPs, were computed. SN, substantia nigra; ROI, region of interest; CAP, coactivation pattern.

Table 1. Demographic, clinical, and neurocognitive characteristics

	FES ($n = 84$)	HC ($n = 94$)	df	Statistics	p value	Effect size
Age (years)	22.62 (6.59)	23.91 (6.14)	176	$t = -1.36$	0.176	Cohen's $d = 0.204$
Sex (Male/Female)	40/44	39/55	1	$\chi^2 = 0.68$	0.411	$\varphi = 0.062$
Education (years)	12.25 (2.43)	14.78 (2.69)	176	$t = -6.55$	<0.001	Cohen's $d = 0.980$
IQ	95.31 (17.91)	114.10 (13.57)	166	$F = 31.31$	<0.001	Partial $\eta^2 = 0.162$
DUP (months)	6 (1; 12)[a]					
PANSS						
Total	90.80 (20.16)					
Positive	14.77 (4.00)					
Negative	20.92 (7.28)					
Disorganized/concrete	9.86 (3.84)					
Excited	9.55 (4.50)					
Depressed	7.52 (3.17)					

FES, first-episode treatment-naïve patients with schizophrenia; HC, healthy control; IQ, intelligence quotient; DUP, duration of untreated psychosis; PANSS, Positive and Negative Syndrome Scale.
Note: values are presented as mean (standard deviation).
[a]Median (quarter; three quarters).

between the two groups, but years of education were lower in FES ($t = -6.549$, $p < 0.001$, Cohen's $d = 0.980$). Additionally, the FES group had lower IQ ($F = 31.31$, $p < 0.001$, Partial $\eta^2 = 0.162$) compared to HCs.

Activity features of SN-relevant CAPs

We identified six CAPs coupled with SN activation (CAP A1 to A6) and six CAPs coupled with SN deactivation (CAP D1 to

D6). According to their activity patterns, these CAPs can be divided into six distinct pairs: CAPs A1—A4, A2—A3, A5—A6, D1—D2, D3—D5, and D4—D6, with each pair containing opposing CAPs but similar connectome features (Fig. 2).

The activated SN-relevant CAPs are shown in Fig. 2a. CAP A1 mainly involved activation in salience/ventral attention network (VAN), SMN, auditory network (AUD), dorsal attention network (DAN), and putamen. CAP A2 was characterized by deactivated VIS and SMN, and activated control network (CON), caudate, thalamus, putamen, pallidum, and brainstem. CAP A3 showed activation in VIS, SMN, DMN, hippocampus, amygdala,

brainstem, and thalamus. CAP A4 mainly included activation in canonical DMN, CON, hippocampus, brainstem, amygdala, and thalamus. CAP A5 was characterized by activation in DAN and CON, and deactivation in DMN and language network (LAN). CAP A6 showed coactivation with SN in DMN, LAN, CON, and widespread subcortical regions, including hippocampus, amygdala, caudate, accumbens, thalamus, brainstem, pallidum, and putamen.

As for deactivated SN-relevant CAPs (Fig. 2b), CAP D1 mainly comprised deactivated DMN, LAN, CON, hippocampus, amygdala, and brainstem. CAP D2 was characterized by activation of
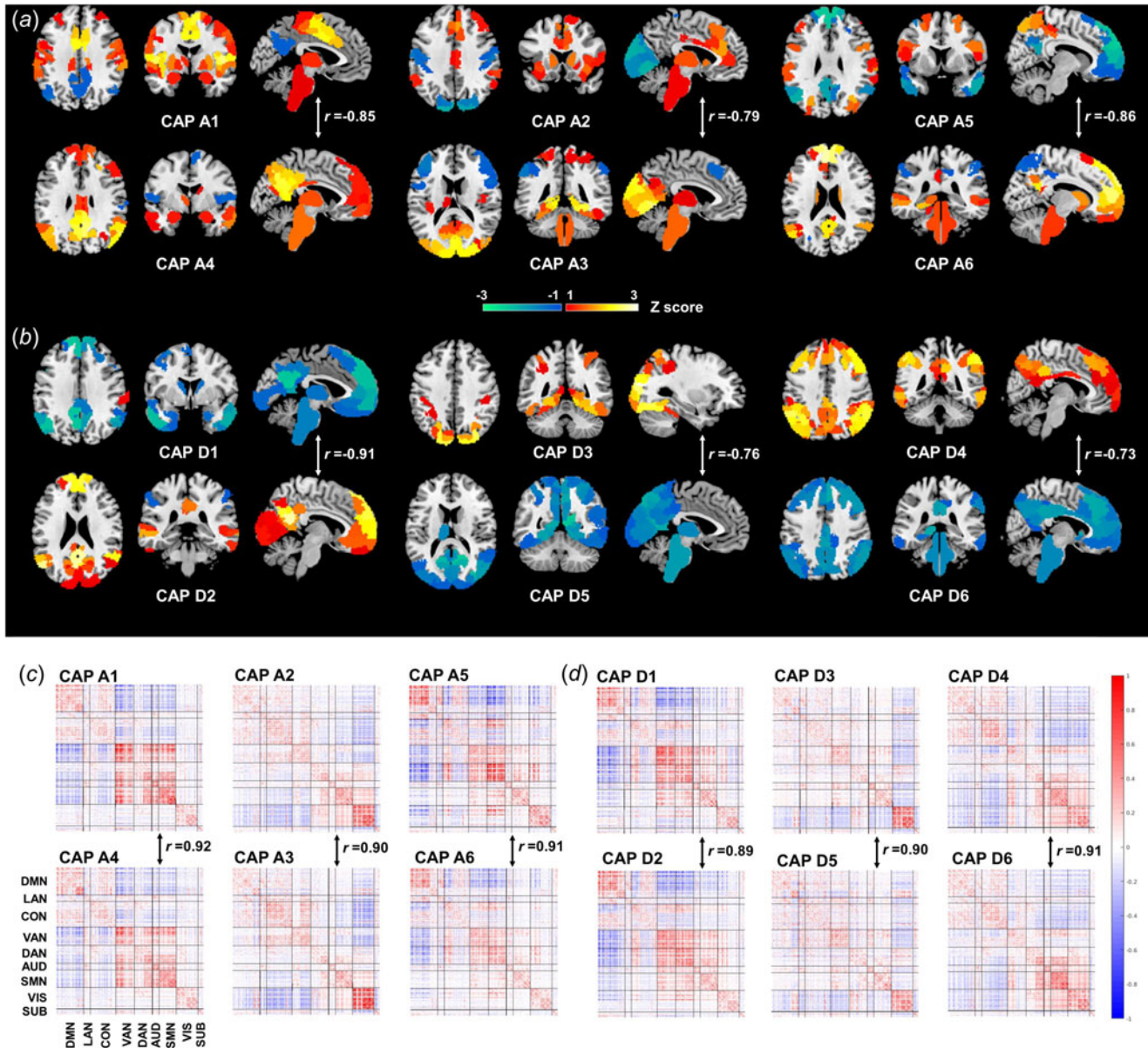

Figure 2. Spatial features of SN-relevant CAPs. According to spatial similarity tests, SN-relevant CAPs could be grouped into six distinct pairs: CAPs A1—A4, A2—A3, A5—A6, D1—D2, D3—D5, and D4—D6, with each pair containing opposing activity patterns but similar connectome profiles. (a) Activity patterns of six SN-activation coupled CAPs and (b) six SN-deactivation coupled CAPs. Regions in warm colors show coactivation whereas regions in cool colors show co-deactivation. To illustrate the brain areas showing significant activity, thresholds of 1 and −1 were used for visualization of each pattern. (c) Connectome maps of six CAPs coupled with SN activation and (d) six CAPs coupled with SN-deactivation. Values in red indicate positive FC, while values in blue indicate negative FC of a pair of ROIs. Spearman's correlation 'r' values are shown in the middle of each pair of CAPs, which represent the spatial similarity between corresponding patterns. SN, substantia nigra; CAP, coactivation pattern; ROI, region of interest; DMN, default mode network; LAN, language network; CON, control network; VAN, salience/ventral attention network; DAN, dorsal attention network; AUD, auditory network; SMN, somatomotor network; VIS, visual network; SUB, subcortex.

DMN, LAN, and CON. CAP D3 contained activated VIS and DAN. CAP D4 mainly included activated CON, DMN, and DAN. CAP D5 involved deactivation in the VIS, DAN, DMN, CON, hippocampus, brainstem, and thalamus. CAP D6 showed deactivation in DMN, CON, VAN, and a number of subcortical structures, involving the thalamus, caudate, brainstem, and accumbens.

See detailed description in online Supplementary Table S1.

Connectome features of SN-relevant CAPs

To further investigate the constructs of CAPs, we depicted the connectome features of SN-relevant CAPs using the edge-centric method (Fig. 2c and 2d). We noticed that each CAP seems to share a similar connectome feature with its opposing CAP. CAPs A1 and A4 mainly showed intra-network positive FCs in VAN, AUD, and SMN, positive internetwork FCs among VAN, DAN, AUD, and SMN, as well as negative FCs between DMN and VAN, DAN, AUD, SMN. CAPs A2 and A3 exhibited strong within-network positive FCs in VIS, and negative FCs between VIS and CON, VAN, and subcortex. CAPs A5 and A6 displayed strong positive FCs within DMN, DAN, and VIS, but negative FCs between DMN and VAN, DAN. CAPs D1 and D2 were largely similar to CAPs A5 and A6 but demonstrated stronger positive FCs within VAN and between VAN and DAN. CAPs D3 and D5 were characterized by prevalent weak whole-brain positive FCs, with the exception of strong positive FCs within VIS and negative FCs between VIS and other networks. CAPs D4 and D6 primarily exhibited positive FCs both within and between SMN and VIS, as well as negative FCs between SMN, VIS, and CON, DMN.

Spatial similarity

We estimated similarities among all CAPs and their connectome maps by computing Spearman's correlation coefficients respectively (online Supplementary Fig. S2). We confirmed that each CAP shared similar connectome features with its corresponding opposing CAP. Across the activated and deactivated states of SN, CAPs showed relatively distinct patterns.

Temporal features of SN-relevant CAPs

Compared to HCs, FES exhibited a significantly lower occurrence of CAP A3 ($F = 7.14$, FDR-corrected $p = 0.030$, Partial $\eta^2 = 0.040$), and a significantly higher occurrence of CAP A6 ($F = 8.54$, FDR-corrected $p = 0.030$, Partial $\eta^2 = 0.047$) (Fig. 3a). During SN deactivation, FES showed an increased occurrence of CAP D3 ($F = 8.09$, FDR-corrected $p = 0.030$, Partial $\eta^2 = 0.045$) and a reduced occurrence of CAP D5 ($F = 6.58$, FDR-corrected $p = 0.034$, Partial $\eta^2 = 0.037$) compared to HCs (Fig. 3b).

We found statistically significant between-group differences in the balance ratios of two pairs of CAPs, which were CAPs A3—A2 ($F = 7.48$, FDR-corrected $p = 0.030$, Partial $\eta^2 = 0.041$) and CAPs D5—D3 ($F = 12.20$, FDR-corrected $p = 0.011$, Partial $\eta^2 = 0.066$) (Fig. 3c). In the case of CAPs A3 and A2, the imbalance was more pronounced towards CAP A2 in FES compared to HCs. For CAPs D5 and D3, FES shifted their balance towards CAP D3, whereas HCs maintained the balance between the two patterns. See detailed results in online Supplementary Table S2. After accounting for IQ as an additional covariate, most of our significant findings remained unchanged, with the notable exception of the occurrence of CAP D5 (online Supplementary Table S3).

Correlation between aberrant temporal dynamics and symptom burden

In FES patients, we noted a suggestive correlation between a higher frequency of CAP A6 and a lower positive factor score of PANSS (including delusions, hallucinations, grandiosity, and unusual thought content items, df = 61, $r = -0.353$, uncorrected $p = 0.005$, Fig. 4a). Adjusting for IQ slightly altered this correlation (df = 55, $r = -0.353$, uncorrected $p = 0.007$). The occurrence of CAP D5 exhibited a marginal positive correlation with DUP (df = 64, $r = 0.247$, uncorrected $p = 0.041$, Fig. 4b), which was attenuated when including IQ as an additional covariate (df = 57, $r = 0.247$, uncorrected $p = 0.051$). However, no correlations survived FDR corrections.

Between-group spatial comparison

Our analysis indicated that the spatial organizations of CAPs were similar across both groups. The similarity estimates for CAPs and connectome maps between the groups ranged from $r = 0.84$ to $r = 0.99$ (see online Supplementary Fig. S3). Further, two-sample t tests on subject-level CAPs revealed no significant differences between the groups after applying FDR correction.

Discussion

In the current study, we revealed rich functional reconfigurations in CAPs under both the activation and deactivation states of SN. We also found that CAPs with opposing activation patterns shared similar connectome profiles. During SN activation, FES demonstrated increased recruitment of CAP A6 (characterized by activated DMN, LAN, CON, caudate, and other subcortical regions) compared to HCs. Furthermore, the balance in a pair of antagonistic CAPs in FES shifted towards a CAP characterized by SN-coactivation with CON, caudate, and thalamus. During SN deactivation, FES exhibited excessive recruitment of CAP D3 (featuring VIS and DAN activation) but insufficient recruitment of its opposing pattern CAP D5. These findings depict a disrupted temporal structure of functional organization related to SN in the early unmedicated stage of schizophrenia.

Dynamic functional reconfigurations under SN activation and deactivation

We observed that the CAPs related to SN activation and deactivation displayed distinct spatial organizations. In all CAPs relevant to SN activation, SN consistently coactivated with most other subcortical structures, especially adjacent regions within the brainstem, dopamine-rich structures (caudate, accumbens) (McCutcheon et al., 2018), the key hub of cortical-subcortical circuitry (thalamus) (Giraldo-Chica & Woodward, 2017), hippocampus, and amygdala. At the cortical level, SN was frequently and strongly coactivated with DMN and CON. Regarding the deactivated-SN state, SN only co-deactivated with other subcortical regions in three of the six deactivation-relevant CAPs, namely CAPs D1, D5, and D6. Meanwhile, SN showed frequent co-deactivation with DMN and CON in these three CAPs. The identified profiles of SN-relevant CAPs partly support the dominance of CAPs involving midline cortical regions in dynamic
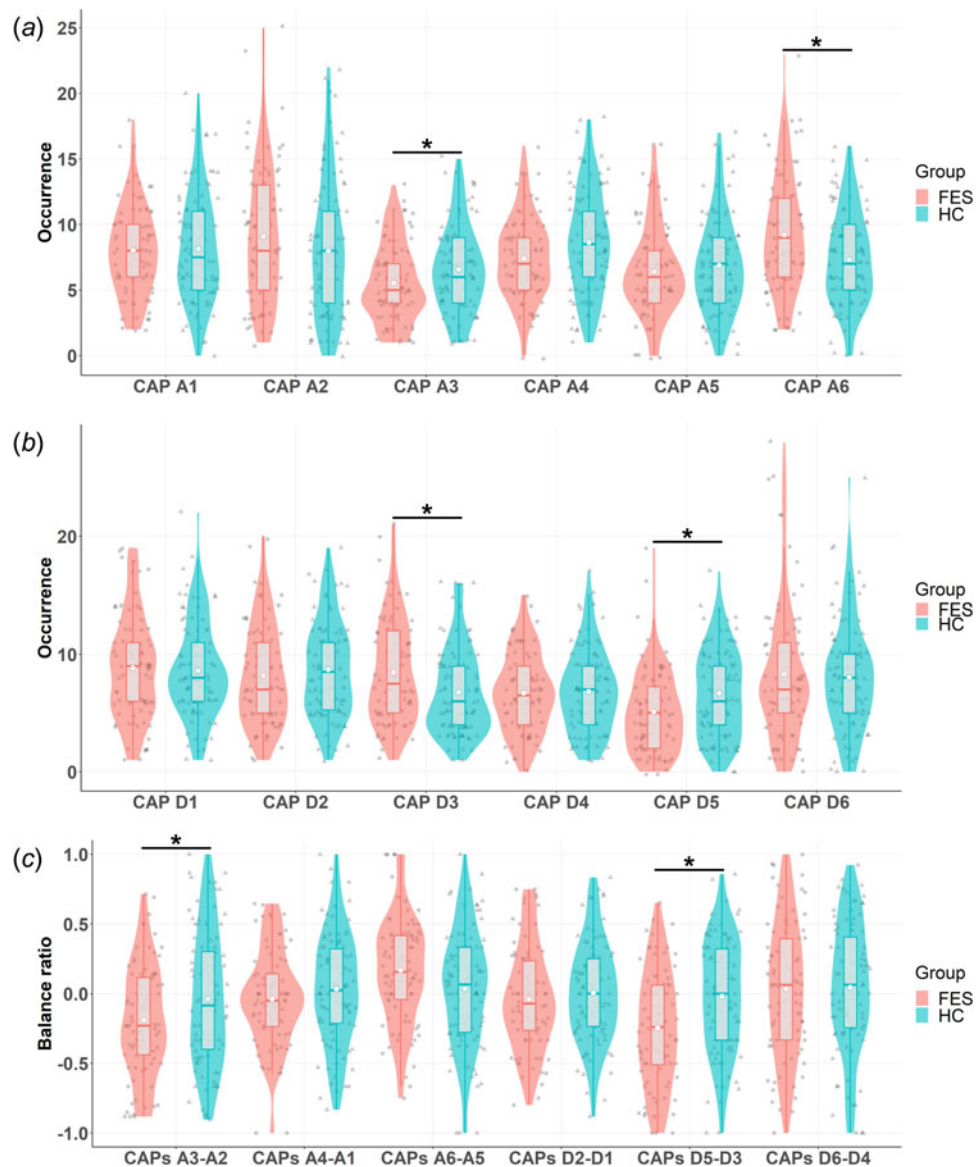
Figure 3. Between-group comparison of temporal features. (a) Statistically significant intergroup differences were found in the occurrence of CAPs A3 and A6 that coupled with SN-activation, (b) as well as in the occurrence of CAPs D3 and D5 that coupled with SN-deactivation. (c) The balance ratio of CAPs A3—A2 and CAPs D5—D3 were significantly reduced in FES. Boxplots represent the means (the white circle), the medians (the line), the upper and lower quartiles (the end of the box), and the highest and lowest values excluding outliers (the extreme lines) of the CAP occurrence or the balance ratio.
Note: *indicates $p < 0.05$, with FDR correction. Abbreviations: CAP, coactivation pattern; SN, substantia nigra; FES, first-episode treatment-naïve patients with schizophrenia; HC, healthy control.

resting-state brain functioning (Janes, Peechatka, Frederick, & Kaiser, 2020). Besides, such rich dynamic reconfigurations support the contribution of SN to brain dynamics. The neuromodulatory effects of dopamine in coordinating network dynamics have been confirmed in previous simultaneous positron emission tomography-fMRI study (Roffman et al., 2016). Specifically, the dopaminergic midbrain nuclei were reported to be functionally integrated with DMN (Bär et al., 2016). Furthermore, dopamine agonists could increase the midbrain-DMN and caudate-CON FCs (Cole et al., 2013b), as well as CON's FCs with basal ganglia network and DMN (Cole et al., 2013a). Other major subcortical structures (thalamus, striatum, amygdala, and hippocampus) also contribute to network dynamics through intra-subcortical communications as well as with cortical areas (Chumin et al.,

2022). Taken together, these findings suggest that SN may play an important role in brain dynamics, which are potentially mediated by changing dopaminergic activities. Moreover, network dynamics possibly involves the coordination between SN and key subcortical structures.

Our findings reveal that CAPs exhibit dynamic and antagonistic organization, often forming pairs with opposing activation patterns. This observation aligns with findings from previous CAP studies (Li et al., 2021; Yang et al., 2021). Intriguingly, through an edge-centric approach, we discovered that these opposing CAPs exhibit highly similar connectome profiles. The connections between brain areas are fundamental to the brain's functional organization and the integration of cognitive functions (Thiebaut de Schotten & Forkel, 2022). Previous research has
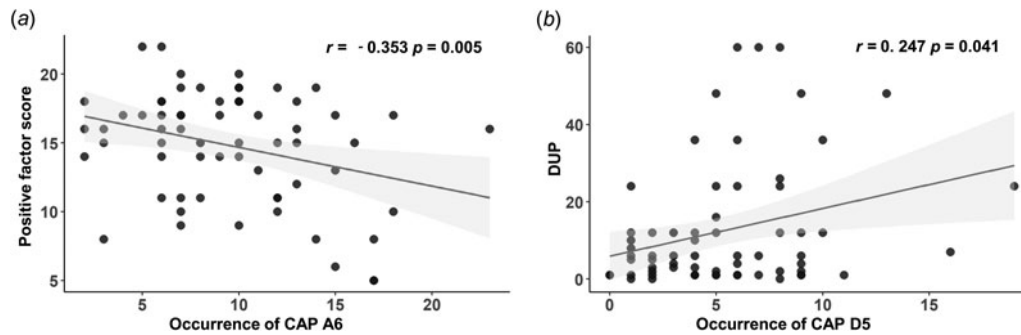
Figure 4. Clinical association of temporal dynamic alterations in FES. (a) The occurrence of CAP A6 displayed a negatively correlated trend with the Positive factor score of PANSS, measured by partial Pearson's correlation adjusting for age, gender, and years of education. (b) The occurrence of CAP D5 showed a trend towards a positive correlation with DUP, assessed by Spearman's correlation after regressing out age, gender, and years of education. The shadow represents the 95% confidence interval of the linear trend.

Note: p values were not FDR corrected. FES, first-episode treatment-naïve patients with schizophrenia; CAP, coactivation pattern; PANSS, Positive and Negative Syndrome Scale; DUP, duration of untreated psychosis.

shown that the activities of specific networks correlate with variations in FCs within and between certain networks, and dynamic changes in FCs may lead to network reconfigurations (Di & Biswal, 2015). Our observations suggest that the antagonistic activity patterns observed in CAPs could be underpinned by common connectome configurations.

Aberrant temporal features of SN-relevant CAPs in FES

In the activated-SN state, we found significantly increased recruitment of CAP A6 and a tilted balance towards CAP A2 against its antagonistic CAP A3 in FES. The classic dopamine hypothesis of schizophrenia mainly emphasizes mesolimbic hyperdopaminergia involving the ventral tegmental area (VTA), but recent neuroimaging meta-analysis has established that the major hyperdopaminergia in schizophrenia happens in the dorsal striatum (containing caudate and putamen), which receives input from SN rather than VTA (McCutcheon et al., 2018, 2019; Stahl, 2021). CAPs A2 and A6 both demonstrated strong SN-coactivation with caudate and secondarily with putamen and pallidum at a lower intensity. The over-recruitment of CAPs A2 and A6 in FES supports and extends the recent notion of the dopamine hypothesis in a temporal dimension. Notably, CAP A6 also involved the coactivation of the amygdala and hippocampus. Previous literature found that stress leads to hyperactivity in the amygdala and subsequently hippocampus (Grace, 2016). The hippocampal overdrive causes increased dopamine neuron firing and a hyper-responsive dopamine state, leading to aberrant salience and psychotic symptoms (Grace, 2016; Winton-Brown, Fusar-Poli, Ungless, & Howes, 2014). Regarding the cortical level, CAP A6 exhibited strong coactivation in DMN, LAN, and CON and CAP A2 displayed SN-coactivation with CON. These large-scale networks were found disrupted in schizophrenia and widely associated with clinical symptoms (Baker et al., 2014, 2019; Li et al., 2017; Whitfield-Gabrieli et al., 2009).

We noted a trend suggesting a correlation between the increased recruitment of CAP A6 and less severe positive symptoms, although this finding did not withstand FDR correction. This observation aligns with recent findings by Li et al., who reported higher gray matter concentration in a network involving frontoparietal and temporal regions (encompassing parts of DMN, LAN, and CON) associated with less severe positive symptoms in FES (Li et al., 2022). This leads us to speculate that

heightened activity in the SN-related striato-thalamo-cortical circuit might represent a compensatory functional reorganization in response to dopaminergic disturbances in schizophrenia, even prior to medication exposure. However, considering the weak and uncorrected nature of the correlation between occurrence of CAP A6 and the severity of positive symptoms, it is clear that more extensive, longitudinal studies with larger sample size are necessary to determine whether SN-related brain dynamics could serve as a marker of resilience contributing to a reduced symptom burden in schizophrenia.

In contrast, during the deactivated-SN state, we observed over-recruitment of CAP D3 but reduced recruitment of CAP D5 in FES, as well as an imbalance between these two CAPs. CAP D5 featured co-deactivation of VIS, DAN, DMN, and CON, whereas CAP D3 exhibited coactivation in VIS and DAN. Elevated baseline extracellular dopamine levels have been reported in schizophrenia, which may be caused by continuously excessive tonic dopamine releases, and facilitate salience dysregulation (Abi-Dargham et al., 2000; Winton-Brown et al., 2014). One possibility is that brain dynamics under SN deactivation in schizophrenia may still be impacted by elevated baseline dopamine levels, which may drive more coactivation of DAN and VIS and lead to the relative predominance of CAP D3. VIS and DAN support visual processing and goal-directed attention respectively (Corbetta & Shulman, 2011; Uddin, Yeo, & Spreng, 2019). The over-recruitment of CAP D3 might contribute to improper allocation of attention to internal thought and emotion (Lefort-Besnard et al., 2018; Winton-Brown et al., 2014) as well as biased visual perception (Li, Sweeney, & Hu, 2020; Türközer et al., 2019), thus providing a potential neuropathological basis for psychotic symptoms such as hallucination and delusion. What's more, we found with longer DUP, the recruitment of CAP D5 tended to increase in FES, which might be a compensatory mechanism conferred by dynamic reconfiguration in unmedicated states. However, the observed imbalance between CAPs D3 and D5 suggests that this compensation would be unsuccessful.

Strength and limitations

To our knowledge, we reported brain dynamic aberrances related to SN at a drug-naïve first-episode stage of a large schizophrenia sample for the first time. Studying drug-naïve patients ensures that observed differences are related to the underlying

pathophysiology of schizophrenia rather than the effects of medication, and also minimizes the influence of disease progression and its potential effects on brain structure and function. Another strength is that our CAP analyses focus on time points with strong links to SN, allowing us to address the dopamine hypothesis of schizophrenia. While the CAP method focuses on activity and the edge-centric model emphasizes connectivity (Preti, Bolton, & Van De Ville, 2017), our work shows that integrating complementary dynamic approaches is likely to enrich the research on spatiotemporal brain organization (Bolton, Morgenroth, Preti, & Van De Ville, 2020a).

There are also a few limitations. Firstly, it is crucial to recognize that the SN-relevant CAPs identified in our study do not establish a causal link between dopamine signaling and brain dynamics, primarily due to the limited temporal resolution of fMRI, which cannot track brain dynamics at the millisecond scale. Nonetheless, existing research has demonstrated that fMRI is capable of capturing neuronal activation signals potentially influenced by transient dopaminergic input (Schultz, 2010; Winton-Brown et al., 2014). Moreover, BOLD signals are known to reflect dynamic changes in neuronal spike rate or the neuromodulatory effects of dopamine (Logothetis, 2008). Given the standard spatial resolution of 3 T fMRI, we utilized a high-resolution SN atlas map and averaged the signal across all voxels in the bilateral SN to optimize anatomical specificity and signal-to-noise ratio. While this study offers important insights into the interplay between the SN and other brain regions, caution should be exercised in interpreting the anatomical specificity of SN-relevant CAPs. Future research in this domain could benefit from employing ultra-high resolution fMRI combined with multiband or parallel acquisition techniques to enhance both spatial and temporal resolution. Additionally, subdividing the SN into the pars compacta and reticulata using high-field fMRI may provide further insights into whether MRI metrics in these SN subregions correlate with specific neuropathological substrate of schizophrenia. Secondly, this work focuses on dopaminergic-SN, but understanding identified dynamic alterations in schizophrenia to what extent are SN specific will require future investigation across multiple neuromodulatory nuclei (van den Brink, Pfeffer, & Donner, 2019). Thirdly, since our research focused on investigating the dynamics of CAPs, we adopted a 6-cluster solution for categorizing SN-related CAPs, enabling us to capture the nuanced and dynamic nature of these patterns. However, we posit that if the clustering procedure were performed basing on connectome features or edges between brain areas, a 3-means solution might emerge, which would suggest a more unified underlying connectome structure among certain CAP pairs. Lastly, from our observation, the spatial between-group differences of CAPs are relatively subtle. Though these results are consistent with a recent CAP study (Wang et al., 2021), more rigorous statistical methods or incorporating graph theory will be required on testing spatial differences in future research.

Conclusion

In summary, we illustrate that the brain exhibited rich functional reconfigurations under both SN activation and deactivation. We demonstrate excessive or insufficient recruitments of specific SN-relevant CAPs in an early unmedicated stage of schizophrenia, which involves dopamine-rich subcortical regions and critical large-scale networks such as DMN, LAN, CON, DAN, and VIS. Such abnormal temporal functional organizations in

schizophrenia are potentially shaped by the dysregulated dopaminergic system involving SN, which enriches the current dopamine hypothesis from a dynamic level. In future research, adopting multimodal approaches within a longitudinal cohort could be highly beneficial. This would enable a more comprehensive understanding of the role of dopamine-relevant brain dynamics in the pathophysiology of schizophrenia.

References

Abi-Dargham, A., Rodenhiser, J., Printz, D., Zea-Ponce, Y., Gil, R., Kegeles, L. S., … Laruelle, M. (2000). Increased baseline occupancy of D2 receptors by dopamine in schizophrenia. *Proceedings of the National Academy of Sciences*, 97(14), 8104–8109. doi: 10.1073/pnas.97.14.8104

Baker, J. T., Dillon, D. G., Patrick, L. M., Roffman, J. L., Brady, R. O., Pizzagalli, D. A., … Holmes, A. J. (2019). Functional connectomics of affective and psychotic pathology. *Proceedings of the National Academy of Sciences*, 116(18), 9050–9059. doi: 10.1073/pnas.1820780116

Baker, J. T., Holmes, A. J., Masters, G. A., Yeo, B. T. T., Krienen, F., Buckner, R. L., & Öngür, D. (2014). Disruption of cortical association networks in schizophrenia and psychotic bipolar disorder. *JAMA Psychiatry*, 71(2), 109–118. doi: 10.1001/jamapsychiatry.2013.3469

Bär, K.-J., de la Cruz, F., Schumann, A., Koehler, S., Sauer, H., Critchley, H., & Wagner, G. (2016). Functional connectivity and network analysis of midbrain and brainstem nuclei. *Neuroimage*, 134, 53–63. doi: 10.1016/j.neuroimage.2016.03.071

Bolton, T. A. W., Morgenroth, E., Preti, M. G., & Van De Ville, D. (2020a). Tapping into multi-faceted human behavior and psychopathology using fMRI brain dynamics. *Trends in Neurosciences*, 43(9), 667–680. doi: 10.1016/j.tins.2020.06.005

Bolton, T. A. W., Tuleasca, C., Wotruba, D., Rey, G., Dhanis, H., Gauthier, B., … Van De Ville, D. (2020b). TbCAPs: A toolbox for co-activation pattern analysis. *Neuroimage*, 211, 116621. doi: 10.1016/j.neuroimage.2020.116621

Bolton, T. A. W., Wotruba, D., Buechler, R., Theodoridou, A., Michels, L., Kollias, S., … Van De Ville, D. (2020c). Triple network model dynamically

revisited: Lower salience network state switching in pre-psychosis. *Frontiers in Physiology*, 11, 66. doi: 10.3389/fphys.2020.00066

Chang, C., & Glover, G. H. (2010). Time–frequency dynamics of resting-state brain connectivity measured with fMRI. *Neuroimage*, 50(1), 81–98. doi: 10.1016/j.neuroimage.2009.12.011

Charlson, F. J., Ferrari, A. J., Santomauro, D. F., Diminic, S., Stockings, E., Scott, J. G., … Whiteford, H. A. (2018). Global epidemiology and burden of schizophrenia: Findings from the global burden of disease study 2016. *Schizophrenia Bulletin*, 44(6), 1195–1203. doi: 10.1093/schbul/sby058

Chen, J. E., Chang, C., Greicius, M. D., & Glover, G. H. (2015). Introducing co-activation pattern metrics to quantify spontaneous brain network dynamics. *Neuroimage*, 111, 476–488. doi: 10.1016/j.neuroimage.2015.01.057

Chinta, S. J., & Andersen, J. K. (2005). Dopaminergic neurons. *The International Journal of Biochemistry & Cell Biology*, 37(5), 942–946. doi: 10.1016/j.biocel.2004.09.009

Christoff, K., Irving, Z. C., Fox, K. C. R., Spreng, R. N., & Andrews-Hanna, J. R. (2016). Mind-wandering as spontaneous thought: A dynamic framework. *Nature Reviews Neuroscience*, 17(11), 718–731. doi: 10.1038/nrn.2016.113

Chumin, E. J., Faskowitz, J., Esfahlani, F. Z., Jo, Y., Merritt, H., Tanner, J., … Sporns, O. (2022). Cortico-subcortical interactions in overlapping communities of edge functional connectivity. *Neuroimage*, 250, 118971. doi: 10.1016/j.neuroimage.2022.118971

Cloutier, M., Sanon Aigbogun, M., Guerin, A., Nitulescu, R., Ramanakumar, A. V., Kamat, S. A., … Wu, E. (2016). The economic burden of schizophrenia in the United States in 2013. *The Journal of Clinical Psychiatry*, 77(06), 764–771. doi: 10.4088/JCP.15m10278

Cole, D. M., Beckmann, C. F., Oei, N. Y. L., Both, S., van Gerven, J. M. A., & Rombouts, S. A. R. B. (2013a). Differential and distributed effects of dopamine neuromodulations on resting-state network connectivity. *Neuroimage*, 78, 59–67. doi: 10.1016/j.neuroimage.2013.04.034

Cole, D. M., Oei, N. Y. L., Soeter, R. P., Both, S., van Gerven, J. M. A., Rombouts, S. A. R. B., & Beckmann, C. F. (2013b). Dopamine-dependent architecture of cortico-subcortical network connectivity. *Cerebral Cortex*, 23(7), 1509–1516. doi: 10.1093/cercor/bhs136

Conio, B., Martino, M., Magioncalda, P., Escelsior, A., Inglese, M., Amore, M., & Northoff, G. (2020). Opposite effects of dopamine and serotonin on resting-state networks: Review and implications for psychiatric disorders. *Molecular Psychiatry*, 25(1), 82–93. doi: 10.1038/s41380-019-0406-4

Corbetta, M., & Shulman, G. L. (2011). Spatial neglect and attention networks. *Annual Review of Neuroscience*, 34, 569–599. doi: 10.1146/annurev-neuro-061010-113731

Desikan, R. S., Ségonne, F., Fischl, B., Quinn, B. T., Dickerson, B. C., Blacker, D., … Killiany, R. J. (2006). An automated labeling system for subdividing the human cerebral cortex on MRI scans into gyral based regions of interest. *Neuroimage*, 31(3), 968–980. doi: 10.1016/j.neuroimage.2006.01.021

Di, X., & Biswal, B. B. (2015). Dynamic brain functional connectivity modulated by resting-state networks. *Brain Structure and Function*, 220(1), 37–46. doi: 10.1007/s00429-013-0634-3

Faskowitz, J., Esfahlani, F. Z., Jo, Y., Sporns, O., & Betzel, R. F. (2020). Edge-centric functional network representations of human cerebral cortex reveal overlapping system-level architecture. *Nature Neuroscience*, 23(12), 1644–1654. doi: 10.1038/s41593-020-00719-y

Friston, K., Brown, H. R., Siemerkus, J., & Stephan, K. E. (2016). The dysconnection hypothesis (2016). *Schizophrenia Research*, 176(2-3), 83–94. doi: 10.1016/j.schres.2016.07.014

Giraldo-Chica, M., & Woodward, N. D. (2017). Review of thalamocortical resting-state fMRI studies in schizophrenia. *Schizophrenia Research*, 180, 58–63. doi: 10.1016/j.schres.2016.08.005

Gong, Y., & Dai, X. (1984). Application of the short forms of Wechsler intelligence scale. *Bulletin of Hunan Medical College*, 9(04), 393–401. Retrieved from https://kns.cnki.net/kcms2/article/abstract?v=3IEynGI71r-voch0KcV6zKP6EqZDxZ9rc5dKo_EdMnOyZhQGC5HDNZigB60NcDBlLXnSq2xyEpVGiy8g7vAdYN_ZONxaBTzAiTHzFOD719eirpiU44a6DRXPy0Jzq9Warex9twJkufE=&uniplatform=NZKPT

Grace, A. A. (2016). Dysregulation of the dopamine system in the pathophysiology of schizophrenia and depression. *Nature Reviews Neuroscience*, 17(8), 524–532. doi: 10.1038/nrn.2016.57

Gu, Z., Schlesner, M., & Hübschmann, D. (2021). cola: An R/Bioconductor package for consensus partitioning through a general framework. *Nucleic Acids Research*, 49(3), e15–e15. doi: 10.1093/nar/gkaa1146

Howes, O. D., & Kapur, S. (2009). The dopamine hypothesis of schizophrenia: Version III--The final common pathway. *Schizophrenia Bulletin*, 35(3), 549–562. doi: 10.1093/schbul/sbp006

Howes, O. D., McCutcheon, R., Owen, M. J., & Murray, R. M. (2017). The role of genes, stress, and dopamine in the development of schizophrenia. *Biological Psychiatry*, 81(1), 9–20. doi: 10.1016/j.biopsych.2016.07.014

Howes, O. D., Williams, M., Ibrahim, K., Leung, G., Egerton, A., McGuire, P. K., & Turkheimer, F. (2013). Midbrain dopamine function in schizophrenia and depression: A post-mortem and positron emission tomographic imaging study. *Brain*, 136(11), 3242–3251. doi: 10.1093/brain/awt264

Hutchison, R. M., Womelsdorf, T., Allen, E. A., Bandettini, P. A., Calhoun, V. D., Corbetta, M., … Chang, C. (2013). Dynamic functional connectivity: Promise, issues, and interpretations. *Neuroimage*, 80, 360–378. doi: 10.1016/j.neuroimage.2013.05.079

Janes, A. C., Peechatka, A. L., Frederick, B. B., & Kaiser, R. H. (2020). Dynamic functioning of transient resting-state coactivation networks in the human connectome project. *Human Brain Mapping*, 41(2), 373–387. doi: 10.1002/hbm.24808

Kay, S. R., Fiszbein, A., & Opler, L. A. (1987). The positive and negative syndrome scale (PANSS) for schizophrenia. *Schizophrenia Bulletin*, 13(2), 261–276. doi: 10.1093/schbul/13.2.261

Keuken, M. C., Bazin, P. L., Crown, L., Hootsmans, J., Laufer, A., Müller-Axt, C., … Forstmann, B. U. (2014). Quantifying inter-individual anatomical variability in the subcortex using 7T structural MRI. *Neuroimage*, 94, 40–46. doi: 10.1016/j.neuroimage.2014.03.032

Kong, R., Yang, Q., Gordon, E., Xue, A., Yan, X., Orban, C., … Yeo, B. T. T. (2021). Individual-specific areal-level parcellations improve functional connectivity prediction of behavior. *Cerebral Cortex*, 31(10), 4477–4500. doi: 10.1093/cercor/bhab101

Lefort-Besnard, J., Bassett, D. S., Smallwood, J., Margulies, D. S., Derntl, B., Gruber, O., … Bzdok, D. (2018). Different shades of default mode disturbance in schizophrenia: Subnodal covariance estimation in structure and function. *Human Brain Mapping*, 39(2), 644–661. doi: 10.1002/hbm.23870

Li, K., Sweeney, J. A., & Hu, X. P. (2020). Context-dependent dynamic functional connectivity alteration of lateral occipital cortex in schizophrenia. *Schizophrenia Research*, 220, 201–209. doi: 10.1016/j.schres.2020.03.020

Li, M., Dahmani, L., Wang, D., Ren, J., Stocklein, S., Lin, Y., … Liu, H. (2021). Co-activation patterns across multiple tasks reveal robust anti-correlated functional networks. *Neuroimage*, 227, 117680. doi: 10.1016/j.neuroimage.2020.117680

Li, M., Deng, W., Li, Y., Zhao, L., Ma, X., Yu, H., … Li, T. (2022). Ameliorative patterns of grey matter in patients with first-episode and treatment-naïve schizophrenia. *Psychological Medicine*, 53(8), 3500–3510. doi: 10.1017/s0033291722000058

Li, T., Wang, Q., Zhang, J., Rolls, E. T., Yang, W., Palaniyappan, L., … Feng, J. (2017). Brain-wide analysis of functional connectivity in first-episode and chronic stages of schizophrenia. *Schizophrenia Bulletin*, 43(2), 436–448. doi: 10.1093/schbul/sbw099

Liu, X., & Duyn, J. H. (2013). Time-varying functional network information extracted from brief instances of spontaneous brain activity. *Proceedings of the National Academy of Sciences*, 110(11), 4392–4397. doi: 10.1073/pnas.1216856110

Liu, X., Zhang, N., Chang, C., & Duyn, J. H. (2018). Co-activation patterns in resting-state fMRI signals. *Neuroimage*, 180(Pt B), 485–494. doi: 10.1016/j.neuroimage.2018.01.041

Logothetis, N. K. (2008). What we can do and what we cannot do with fMRI. *Nature*, 453(7197), 869–878. doi: 10.1038/nature06976

Marder, S. R., Ropper, A. H., & Cannon, T. D. (2019). Schizophrenia. *New England Journal of Medicine*, 381(18), 1753–1761. doi: 10.1056/NEJMra1808803

Martino, M., Magioncalda, P., Yu, H., Li, X., Wang, Q., Meng, Y., … Li, T. (2018). Abnormal resting-state connectivity in a substantia nigra-related striato-thalamo-cortical network in a large sample of first-episode drug-naïve patients with schizophrenia. *Schizophrenia Bulletin*, 44(2), 419–431. doi: 10.1093/schbul/sbx067

McCutcheon, R. A., Abi-Dargham, A., & Howes, O. D. (2019). Schizophrenia, dopamine and the striatum: From biology to symptoms. *Trends in Neurosciences*, *42*(3), 205–220. doi: 10.1016/j.tins.2018.12.004

McCutcheon, R., Beck, K., Jauhar, S., & Howes, O. D. (2018). Defining the locus of dopaminergic dysfunction in schizophrenia: A meta-analysis and test of the mesolimbic hypothesis. *Schizophrenia Bulletin*, *44*(6), 1301–1311. doi: 10.1093/schbul/sbx180

McKenna, P. J. (1987). Pathology, phenomenology and the dopamine hypothesis of schizophrenia. *British Journal of Psychiatry*, *151*(3), 288–301. doi: 10.1192/bjp.151.3.288

Monti, S., Tamayo, P., Mesirov, J., & Golub, T. (2003). Consensus clustering: A resampling-based method for class discovery and visualization of gene expression microarray data. *Machine Learning*, *52*(1/2), 91–118. doi: 10.1023/a:1023949509487

Owen, M. J., Sawa, A., & Mortensen, P. B. (2016). Schizophrenia. *The Lancet*, *388*(10039), 86–97. doi: 10.1016/s0140-6736(15)01121-6

Power, J. D., Barnes, K. A., Snyder, A. Z., Schlaggar, B. L., & Petersen, S. E. (2012). Spurious but systematic correlations in functional connectivity MRI networks arise from subject motion. *Neuroimage*, *59*(3), 2142–2154. doi: 10.1016/j.neuroimage.2011.10.018

Preti, M. G., Bolton, T. A. W., & Van De Ville, D. (2017). The dynamic functional connectome: State-of-the-art and perspectives. *Neuroimage*, *160*, 41–54. doi: 10.1016/j.neuroimage.2016.12.061

Roffman, J. L., Tanner, A. S., Eryilmaz, H., Rodriguez-Thompson, A., Silverstein, N. J., Ho, N. F., … Catana, C. (2016). Dopamine D1 signaling organizes network dynamics underlying working memory. *Science Advances*, *2*(6), e1501672. doi: 10.1126/sciadv.1501672

Rousseeuw, P. J. (1987). Silhouettes: A graphical aid to the interpretation and validation of cluster analysis. *Journal of Computational and Applied Mathematics*, *20*, 53–65. doi: 10.1016/0377-0427(87)90125-7

Schopp, L. H., Callahan, C. D., Johnstone, B., & Schwake, C. J. (1998). Utility of a seven-subtest version of the WAIS-R among an Alzheimer's disease sample. *Archives of Clinical Neuropsychology*, *13*(7), 637–643. Retrieved from https://www.ncbi.nlm.nih.gov/pubmed/14590625

Schultz, W. (2010). Dopamine signals for reward value and risk: Basic and recent data. *Behavioral and Brain Functions*, *6*(1), 24. doi: 10.1186/1744-9081-6-24

Şenbabaoğlu, Y., Michailidis, G., & Li, J. Z. (2014). Critical limitations of consensus clustering in class discovery. *Scientific Reports*, *4*(1), 6207. doi: 10.1038/srep06207

Sporns, O., Faskowitz, J., Teixeira, A. S., Cutts, S. A., & Betzel, R. F. (2021). Dynamic expression of brain functional systems disclosed by fine-scale analysis of edge time series. *Network Neuroscience*, *5*(2), 405–433. doi: 10.1162/netn_a_00182

Sporns, O., Tononi, G., & Kötter, R. (2005). The human connectome: A structural description of the human brain. *PLoS Computational Biology*, *1*(4), e42. doi: 10.1371/journal.pcbi.0010042

Stahl, S. M. (2021). Psychosis, schizophrenia, and the neurotransmitter networks dopamine, serotonin, and glutamate. In S. M. Stahl (Ed.), *Stahl's essential psychopharmacology* (5th ed., pp. 77–158). Cambridge: Cambridge University Press.

Thiebaut de Schotten, M., & Forkel, S. J. (2022). The emergent properties of the connected brain. *Science (New York, N.Y.)*, *378*(6619), 505–510. doi: 10.1126/science.abq2591

Türközer, H. B., Hasoğlu, T., Chen, Y., Norris, L. A., Brown, M., Delaney-Busch, N., … Öngür, D. (2019). Integrated assessment of visual perception abnormalities in psychotic disorders and relationship with clinical characteristics. *Psychological Medicine*, *49*(10), 1740–1748. doi: 10.1017/s0033291718002477

Uddin, L. Q., Yeo, B. T. T., & Spreng, R. N. (2019). Towards a universal taxonomy of macro-scale functional human brain networks. *Brain Topography*, *32*(6), 926–942. doi: 10.1007/s10548-019-00744-6

van den Brink, R. L., Pfeffer, T., & Donner, T. H. (2019). Brainstem modulation of large-scale intrinsic cortical activity correlations. *Frontiers in Human Neuroscience*, *13*, 340. doi: 10.3389/fnhum.2019.00340

Vita, A., De Peri, L., Deste, G., Barlati, S., & Sacchetti, E. (2015). The effect of antipsychotic treatment on cortical gray matter changes in schizophrenia: Does the class matter? A meta-analysis and meta-regression of longitudinal magnetic resonance imaging studies. *Biological Psychiatry*, *78*(6), 403–412. doi: 10.1016/j.biopsych.2015.02.008

Vita, A., De Peri, L., Deste, G., & Sacchetti, E. (2012). Progressive loss of cortical gray matter in schizophrenia: A meta-analysis and meta-regression of longitudinal MRI studies. *Translational Psychiatry*, *2*(11), e190–e190. doi: 10.1038/tp.2012.116

Wallwork, R. S., Fortgang, R., Hashimoto, R., Weinberger, D. R., & Dickinson, D. (2012). Searching for a consensus five-factor model of the positive and negative syndrome scale for schizophrenia. *Schizophrenia Research*, *137*(1-3), 246–250. doi: 10.1016/j.schres.2012.01.031

Wang, D., Peng, X., Pelletier-Baldelli, A., Orlov, N., Farabaugh, A., Nasr, S., … Holt, D. J. (2021). Altered temporal, but intact spatial, features of transient network dynamics in psychosis. *Molecular Psychiatry*, *26*(6), 2493–2503. doi: 10.1038/s41380-020-00983-1

Whitfield-Gabrieli, S., Thermenos, H. W., Milanovic, S., Tsuang, M. T., Faraone, S. V., McCarley, R. W., … Seidman, L. J. (2009). Hyperactivity and hyperconnectivity of the default network in schizophrenia and in first-degree relatives of persons with schizophrenia. *Proceedings of the National Academy of Sciences*, *106*(4), 1279–1284. doi: 10.1073/pnas.0809141106

Winton-Brown, T. T., Fusar-Poli, P., Ungless, M. A., & Howes, O. D. (2014). Dopaminergic basis of salience dysregulation in psychosis. *Trends in Neurosciences*, *37*(2), 85–94. doi: 10.1016/j.tins.2013.11.003

Yan, C.-G., & Zang, Y.-F. (2010). DPARSF: A MATLAB toolbox for "pipeline" data analysis of resting-state fMRI. *Frontiers in System Neuroscience*, *4*, 13. doi: 10.3389/fnsys.2010.00013

Yang, H., Zhang, H., Di, X., Wang, S., Meng, C., Tian, L., & Biswal, B. (2021). Reproducible coactivation patterns of functional brain networks reveal the aberrant dynamic state transition in schizophrenia. *Neuroimage*, *237*, 118193. doi: 10.1016/j.neuroimage.2021.118193

Zhang, X., Zhang, Y., Liao, J., Jiang, S., Yan, J., Yue, W., … Yan, H. (2018). Progressive grey matter volume changes in patients with schizophrenia over 6 weeks of antipsychotic treatment and their relationship to clinical improvement. *Neuroscience Bulletin*, *34*(5), 816–826. doi: 10.1007/s12264-018-0234-6